# Tunable far infrared laser spectroscopy of van der Waals bonds: Extended measurements on the lowest Σ bend of ArHCl

Kerry L. Busarow, Geoffrey A. Blake,[a] K. B. Laughlin, R. C. Cohen, Y. T. Lee, and R. J. Saykally

*Department of Chemistry and Materials and Chemical Sciences Division, University of California and Lawrence Berkeley Laboratories, Berkeley, California 94720*

(Received 23 February 1988; accepted 18 April 1988)

A tunable far infrared laser system has been used to measure the vibration–rotation spectrum of the lowest Σ bending state of ArHCl near 24 $cm^{-1}$ in a cw planar jet operating with a terminal jet temperature near 3 K. Over 60 transitions have been observed for both $^{35}Cl$ and $^{37}Cl$ isotopes with resolution of the quadrupole hyperfine structure. An improved set of molecular parameters was determined, including *B*, *D*, *H*, and *eqQ* for both upper and lower states. Very narrow linewidths (approximately 300 kHz) resulting in high resolution and sensitivity make this technique a powerful new method for the detailed investigation of intermolecular forces.

## INTRODUCTION

There is a great deal of current interest in the study of weakly bound van der Waals clusters. Much of this activity has been stimulated by recent advances in experimental and theoretical techniques designed to address these systems. Methods now exist for measuring spectroscopic transitions in weakly bound complexes from the microwave through UV-visible frequencies. These techniques are yielding much detailed information regarding the structures and dynamics of complexes, and are revealing subtle features of van der Waals forces never before accessible by either theory or experiment. Clearly, this type of information ultimately contributes a great deal to our general understanding of condensed phase systems.

ArHCl has become the prototype for the study of anisotropic van der Waals interactions. The reason is that it is accessible from both theoretical and experimental approaches, while still exhibiting a substantial degree of complexity as a result of the strong anisotropy of the intermolecular potential. There have been numerous investigations of this system. The earliest studies were performed using static gas cells and low resolution infrared spectroscopy. It was observed that in the null gap between $P(1)$ and $R(0)$ of the HCl vibration–rotation spectrum ($\sim$2900 $cm^{-1}$), extra peaks appeared, which could be attributed to ArHCl and $(HCl)_2$.[1–4] Shortly thereafter, matrix IR studies probed the same region.[5–8] Low resolution far infrared spectroscopy studies were carried out in the wavelength interval between the $J = 1 \leftarrow 0$ and $2 \leftarrow 1$ lines of the pure rotational spectrum of HCl using both matrix techniques[9,10] and static gas cells.[11–13] Differential cross sections from molecular beam elastic scattering experiments provided a value for the isotropic well depth and an isotropic intermolecular potential surface.[14–16]

The most informative studies have been those utilizing high resolution spectroscopic techniques. Most of these investigations used supersonic molecular beams to generate high densities of rotationally cold complexes. Molecular beam electric resonance (MBER) spectroscopy first determined ground state properties from the pure rotational spectrum of ArHCl.[17–19] High resolution laser spectroscopy has been used to study vibrational bands occurring in the near infrared region.[20] These transitions are combination bands of the high frequency HCl stretching vibration and low frequency van der Waals vibrations.

The advantage of high resolution far infrared studies is that the van der Waals vibrations are probed directly, without the additional complications caused by simultaneous high frequency vibrational excitation. The first high resolution FIR spectrum of ArHCl was recorded by Marshall *et al.* using MBER detection.[21] In their study, hyperfine-resolved components of vibration–rotation transitions between the ground state and the lowest Π bending state were probed near 34 $cm^{-1}$, but the inherently low sensitivity of this otherwise elegant method precluded more extensive measurements. Shortly thereafter, Ray *et al.*[22] measured a greatly expanded set of transitions in this same vibration–rotation band using intracavity FIR laser absorption spectroscopy. More recently, Robinson *et al.* measured extended spectra for the Π bend[23] as well as for the two other lowest frequency vibrations, the Σ bend (24 $cm^{-1}$)[24] and the Σ stretch (32 $cm^{-1}$).[25]

In addition to these experimental investigations, there has been considerable theoretical work carried out on the ArHCl system.[15,26–30] In particular, the very important work of Hutson and Howard has provided potential surfaces and spectroscopic predictions which have greatly facilitated spectroscopic investigations. *Ab initio* calculations of potential surfaces have also been performed at a fairly high level of theory, but these are not expected to be reliable at the level of precision required for high resolution spectroscopy.[31]

In this paper we describe a new technique for studying low frequency vibration–rotation transitions in weakly bound complexes with very high resolution, discuss its application for greatly extended measurements of the Σ bending vibration of ArHCl, and elaborate on the preliminary results

[a] Berkeley Miller Postdoctoral Fellow. Present address: Center for Cosmochemistry and Geochemistry, Division of Geology and Planetary Sciences, California Institute of Technology, Pasadena, CA 91125.

 0021-9606/88/151268-09$02.10 

reported elsewhere.[32] This new method involves a combination of two relatively new techniques. A tunable far infrared laser is used to probe ArHCl complexes produced in a continuous planar supersonic jet expansion. The advantage of the continuous planar jet is that it provides a long path length for the light absorption as well as an order of magnitude reduction in the Doppler width relative to a conventional circular nozzle, and operates with a 100% duty cycle. The obvious disadvantage is that this nozzle design requires large vacuum pumps for continuous operation. This difficulty can be overcome to some extent by pulsing the nozzle, thereby reducing the duty cycle and consequent load on the vacuum pumps. Pulsed planar nozzles have been developed by several groups for use in spectroscopic applications,[33,34] and the recent studies by Nesbitt and co-workers are particularly noteworthy.[35] Some additional investigations have been carried out on continuous planar jets, primarily to characterize them.[36–38] In the present experiment, we operate a 1.5 in. long slit nozzle continuously, using a large Roots blower (2600 cfm) to pump the system.

The evolution of tunable far infrared lasers is a very recent development.[39–41] FIR laser spectroscopy has previously involved the use of fixed frequency optically pumped FIR lasers combined with either Stark or Zeeman tuning of the energy levels of the species of interest (see, e.g., Ref. 23). In these experiments, the requirement for strong tuning fields seriously complicates the observed spectra, and often makes spectral assignments difficult. Also, the extent to which the molecular energy levels can be tuned is usually quite limited, requiring the rather tedious employment of numerous FIR laser lines in order to obtain the spectrum. The development of tunable far infrared lasers now permits spectroscopy to be carried out in the absence of these strong perturbing fields with both high sensitivity and high resolution, and with substantially enhanced generality and versatility. This has been demonstrated by our recent observation of the tunneling–rotation and vibration–rotation spectra of $(HCl)_2$ [42] and $ArH_2O$.[43]

## EXPERIMENTAL

A schematic diagram of the experimental arrangement is shown in Fig. 1. The tunable FIR laser system has been described elsewhere[44] in conjunction with studies of molecular ions and will only be discussed briefly here. A 150 W, discharge pumped, cw $CO_2$ laser (Apollo model 150) is used to optically pump a 2.5 m far infrared laser. A large number ($>65$) of simple organic molecules can be pumped to produce over 2000 laser frequencies from 10–200 $cm^{-1}$.[45] In the present experiments, formic acid was used for the production of the 432 and 394 $\mu$m laser lines. The narrow band FIR laser output, approximately 100 kHz FWHM,[46] is directed through a polarizing Michelson diplexer into a cornercube in which a GaAs Shottky barrier diode is mounted. The FIR laser output is coupled onto the diode through a small (0.001 in. diameter) whisker antenna contacting the diode. Tunable microwave radiation (2–75 GHz) is also coupled onto the diode, either directly through the whisker mount or through the post on which the diode is mounted. The FIR and microwave radiation are mixed in the diode and sidebands are produced at the sum and difference of the microwave and the FIR laser frequencies. Therefore, tunable sidebands are generated from 2 to 75 GHz on either side of the laser frequency, yielding a 5 $cm^{-1}$ range of tunability for each FIR laser line. Both the FIR laser frequency and the sidebands radiate from the cornercube, and the sidebands are separated from the much more intense FIR carrier by the diplexer. The sidebands are then collimated and directed through the plane of the supersonic jet and detected using an InSb hot electron bolometer. The FIR laser beam is approximately 1 cm in diameter at the nozzle. The microwave radi-

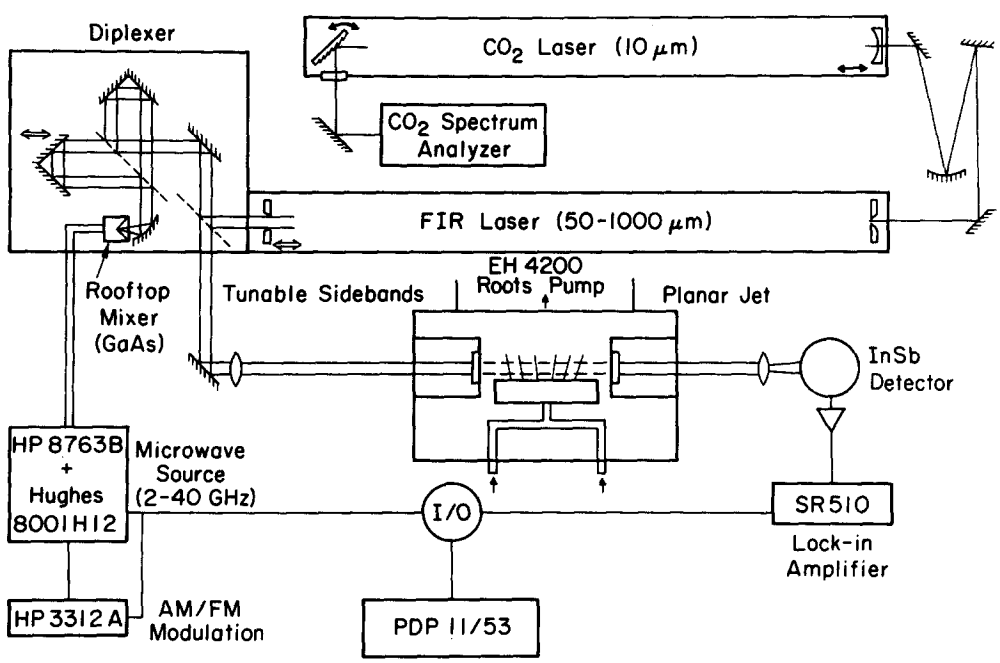


FIG. 1. Tunable far infrared laser/planar supersonic jet apparatus.

ation is frequency modulated at 50 kHz with a deviation of approximately 125 kHz, which results in a corresponding frequency modulation of the sidebands. Lock-in detection is referenced at twice the modulation frequency, producing second derivative line shapes. A PDP11/53 is used to control the experiment and to manipulate the data.

ArHCl was formed in 1%–3% mixtures of HCl in Ar expanded continuously from a 500 Torr backing pressure into a 120 mTorr chamber pressure. The chamber is pumped by a 2600 cfm Roots blower (Edwards EH4200) which is backed by two 145 cfm two-stage mechanical pumps (Edwards E2M275). The pumps are connected to the chamber through 40 ft of 8 in. PVC pipe, reducing the pumping speed to approximately 1600 cfm. The planar nozzle, shown in Fig. 2, is constructed from a rectangular block of stainless steel (2 in. $\times$ 1 in. $\times$ 1 in.), through the length of which a 0.5 in. diameter hole is drilled to hollow out the block. Caps were then welded on the ends, and a hole was drilled through the back side for the gas inlet line. A 1.5 in. $\times$ 0.25 in. slot was milled through the front side. Four blind tapped holes were drilled on either side of the slot for mounting the plates which formed the slit. These two stainless steel plates are 0.125 in. thick, except on the edge that forms the slit, where it is tapered down to a thickness of 0.031 in. The separation of the plates is established by using 0.001 in. shims. Hence, the size of the slit is 1.5 in. $\times$ 0.001 in.

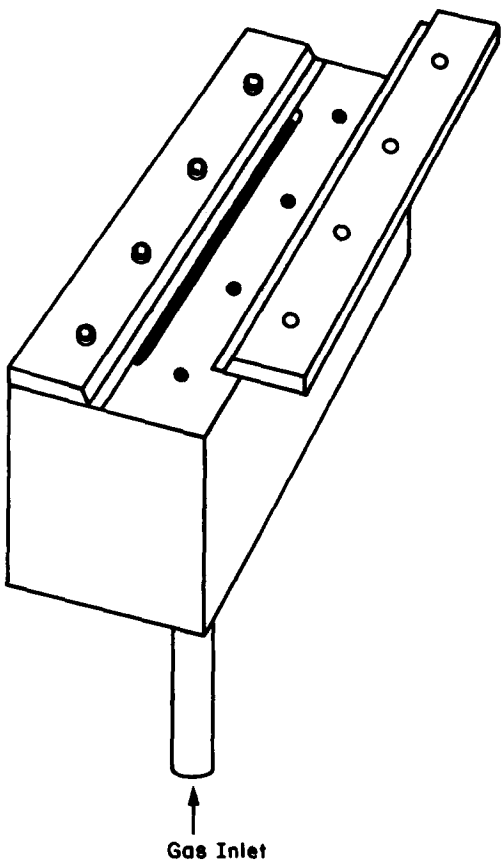


FIG. 2. Planar jet nozzle, drawn to scale, the length of the longest side is 2 in.

There is no gasket between the block and the plates. The surfaces of each plate and the nozzle block are polished to a mirror finish. The nozzle can be readily cooled to 77 K with liquid nitrogen. However, this cooling did not improve the ArHCl signals, therefore the nozzle was operated without temperature control in the present study.

## RESULTS AND ANALYSIS

### Spectra

A total of 61 transitions for $ArH^{35}Cl$ and 63 transitions for $ArH^{37}Cl$ were measured for the lowest $\Sigma$ bend. The optimum S/N was 2000, obtained for $P(3)$ of $ArH^{35}Cl$ (Fig. 3), while the typical S/N is approximately 200. Due to the fact that the FIR laser frequency undergoes a slow drift, it is necessary to calibrate the absorption frequencies using a standard reference gas. The HCl $J = 1 \leftarrow 0$ rotational transition was chosen as the reference and was measured in the jet expansion to obtain a narrower linewidth than in a gas cell. The value of the frequency used for this transition was taken from DeLucia *et al.* and has an uncertainty of approximately 20 kHz.[47] The HCl transition was measured, followed imme-

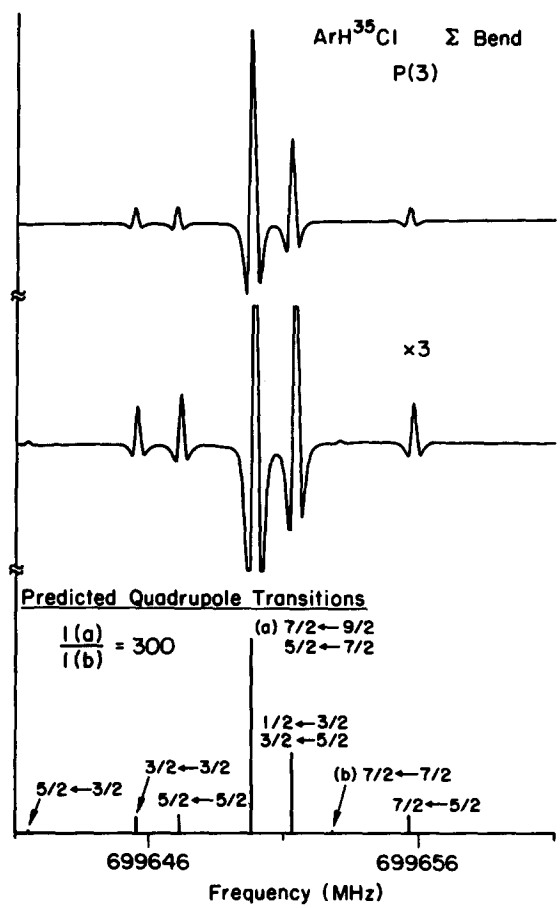


FIG. 3. $P(3)$ of $ArH^{35}Cl$. In the lowest scan the sensitivity is increased by a factor of 3 to show the smallest hyperfine components. The bottom graph shows the predicted hyperfine structure with the intensities. The smallest components, $5/2 \leftarrow 3/2$ and $7/2 \leftarrow 5/2$, are too small to be seen on this scale. The predicted intensity ratio of the largest central peak, labeled (a), to the smallest peak, labeled (b), is 300:1. The overall S/N of this, our best scan, is 2000. ($\tau = 1$ s.)

diately by the measurement of $P(10)$ of $ArH^{35}Cl$, thereby calibrating that peak. The remainder of the ArHCl transitions, both the Cl-35 and the Cl-37 isotopes were then referenced to $P(10)$. The $P(10)$ transition of $ArH^{35}Cl$ is measured using the 692 GHz HCOOH far infrared laser line. Those ArHCl transitions on this laser line are referenced directly to $P(10)$, measuring $P(10)$ before and after each line measurement. Those transitions measured on the 761 GHz HCOOH laser line must be referenced to a line accessible from both laser lines and previously referenced to $P(10)$, such as a lower $R$ branch line. This calibration procedure allowed us to obtain reproducibilities on the order of 50 kHz or less for the FIR transition frequencies. Each peak was also measured twice with up–down scanning to minimize any line shifts caused by time constant effects.

Also included in the fit were rotational transition frequencies measured in the microwave region by Novick and co-workers.[17,19] However, only those transitions measured with better than $\sim 100$ kHz uncertainties were included. A list of all of the transitions used in the fit is given in Table I.

The Hamiltonian used to fit the FIR data was of the standard form appropriate for a linear triatomic molecule, including the effects of nuclear quadrupole hyperfine structure:

$$H = \nu(v+1/2) + B(02^00)J'(J'+1) - D(02^00)[J'(J'+1)]^2 + H(02^00)[J'(J'+1)]^3 + L(02^00)[J'(J'+1)]^4 - eqQ(02^00)[3/4C'(C'+1) - I(I+1)J'(J'+1)]/[2I(2I-1) \times (2J'-1)(2J'+3)] - B(000)J''(J''+1) + D(000)[J''(J''+1)]^2 - H(000)[J''(J''+1)]^3 - L(000) \times [J''(J''+1)]^4 + eqQ(000)[(3/4C''(C''+1) - I(I+1)J''(J''+1)]/[2I(2I-1)(2J''-1)(2J''+3)], \quad (1)$$

where

$$C' = F'(F'+1) - I(I+1) - J'(J'+1),$$

$$C'' = F''(F''+1) - I(I+1) - J''(J''+1),$$

and

$$F = I+J, I+J-1, \ldots, |I-J|.$$

We have obtained values for the rotational constants of the upper and lower states, as well as for the quartic and sextic centrifugal distortion constants ($D$ and $H$) for both vibrational states (Table II). The next higher (octic) centrifugal distortion constant ($L$) was also included in the preliminary analysis. Including $L$ improved the standard deviation of the fit by about 25% for both the Cl-35 and Cl-37 isotopes. In the Cl-35 case, however, it was not possible to meaningfully determine $L$ for the ground state; therefore, $L$ was not included in the final fits. Our values of $B$, $D$, and $H$ for the ground state are slightly more precise than the results obtained by microwave spectroscopy.[19] Although the single line measurement precision of microwave spectroscopy generally exceeds that of the present experiment by approximately a factor of 10, we were able to measure much higher values of $J$ (up to $J = 23$), which allowed us to better determine these constants. For the upper state, the present values of the determined constants are more precise than previous results from FIR laser Stark spectroscopy due to the combined effects of smaller linewidths, measuring to higher $J$, and careful calibration of the observed transitions.

Both chlorine isotopes have nuclear spins of 3/2 and quadrupole splittings were observed in both cases for transitions involving $J \leqslant 5$. Our values for the quadrupole coupling constants are not as precise as the $ArH^{35}Cl$ ground state value obtained from MBER studies.[18] The energy level splittings resulted from the nuclear quadrupole interactions decrease rapidly with increasing $J$; hence there is no advantage in measuring high values of $J$ because hyperfine splittings are observable only up to $J = 5$ or 6, the $P(6)$ splitting for Cl-37 was resolvable but for $R(6)$ it was not resolvable. Therefore, in the Cl-35 fit, the ground state quadrupole coupling constant, $eqQ$, was fixed at the MBER value. Between $J = 6$ and $J = 8$, the quadrupole structure is blended and broadens the peaks significantly, this makes accurate determination of the line centers more difficult. Therefore, $P(7)$, $P(8)$, $P(9)$, $R(6)$, $R(7)$, $R(8)$, are not included in either fit. This improves the overall standard deviation of the fit slightly. Of the lines not listed in Table I, several lines, including $P(5)$, $P(6)$, and $R(11)$ of $ArH^{35}Cl$ and $P(5)$ of $ArH^{37}Cl$, lie within 2 GHz of the FIR laser frequency and cannot be observed. Moreover, $R(9)$ of both isotopes and $R(11)$ of $ArH^{37}Cl$ are close to an atmospheric water absorption line at 752 GHz, which absorbs most of the available laser power, precluding their measurement. The fit deteriorates at high $J$, because above $J = 16$, the single peaks begin to split into Doppler doublets, as will be discussed in a later section. The center frequency of these split peaks is used in the fit, which may result in a somewhat larger error. The standard deviation of the fit is very good for FIR spectroscopy ($\sim 1$ part in $10^7$). The $ArH^{37}Cl$ fit is actually about a factor of 3 better than that of $ArH^{35}Cl$, in part due to the fact that we did not measure to as high a value of $J$, where the fit tends to deteriorate. This does not, however, account for the entire factor of 3 difference.

### Linewidths

It was shown by Veeken and Reuss[34] and more recently by Lovejoy and Nesbitt[35] that the absorption linewidths are substantially reduced in a planar free jet expansion compared with those observed with a circular nozzle jet. In a planar jet, the expansion along the slit is inhibited which results in a reduction in the Doppler broadening when the measurements are carried out with the laser beam propagated parallel to the long slit. In the present experiment, the measured linewidths are approximately ten times smaller than for the case of a circular nozzle, and approximately three times smaller than those found in a room temperature low pressure gas cell. Linewidths of transitions occurring

TABLE I. List of all lines measured for the ArHCl Σ bending vibration. Those lines which do not have an associated obs − calc value were not included in the fit.

| Chlorine-35 measured lines | | | | |
|---|---|---|---|---|
| I | Line | F′←F″ | OBS (MHz) | OMC (kHz) |
| 1 | *P*(23) | | 671 708.028 | − 230 |
| 2 | *P*(22) | | 671 842.823 | 172 |
| 3 | *P*(21) | | 672 079.177 | 216 |
| 4 | *P*(20) | | 672 424.272 | 5 |
| 5 | *P*(19) | | 672 885.192 | 60 |
| 6 | *P*(18) | | 673 467.576 | − 55 |
| 7 | *P*(17) | | 674 177.279 | − 94 |
| 8 | *P*(16) | | 675 019.387 | − 128 |
| 9 | *P*(15) | | 675 998.665 | − 124 |
| 10 | *P*(14) | | 677 119.446 | − 65 |
| 11 | *P*(13) | | 678 385.638 | 30 |
| 12 | *P*(12) | | 679 800.702 | 79 |
| 13 | *P*(11) | | 681 367.791 | 54 |
| 14 | *P*(10) | | 683 089.872 | 93 |
| 15 | *P*( 9) | | 684 969.337 | |
| 16 | *P*( 8) | | 687 008.387 | |
| 17 | *P*( 7) | | 689 208.849 | |
| 18 | *P*( 4) | 4.50←5.50 | 696 792.406 | 10 |
| 19 | *P*( 3) | 3.50←4.50 | 699 650.823 | − 15 |
| 20 | *P*( 2) | 1.50←0.50 | 702 665.329 | − 105 |
| 21 | *P*( 2) | 1.50←1.50 | 702 671.114 | − 82 |
| 22 | *P*( 2) | 2.50←3.50 | 702 675.239 | − 68 |
| 23 | *P*( 2) | 0.50←0.50 | 702 675.790 | − 6 |
| 24 | *P*( 2) | 2.50←2.50 | 702 681.222 | 152 |
| 25 | *P*( 2) | 0.50←1.50 | 702 681.564 | 5 |
| 26 | *P*( 1) | 1.50←0.50 | 705 860.894 | − 58 |
| 27 | *P*( 1) | 1.50←2.50 | 705 865.520 | − 42 |
| 28 | *P*( 1) | 1.50←1.50 | 705 871.236 | − 88 |
| 29 | *R*( 0) | 1.50←1.50 | 712 741.503 | − 28 |
| 30 | *R*( 0) | 2.50←1.50 | 712 747.239 | − 49 |
| 31 | *R*( 0) | 0.50←1.50 | 712 751.972 | 78 |
| 32 | *R*( 1) | 1.50←0.50 | 716 427.603 | − 40 |
| 33 | *R*( 1) | 2.50←2.50 | 716 428.039 | − 102 |
| 34 | *R*( 1) | 1.50←2.50 | 716 432.270 | 16 |
| 35 | *R*( 1) | 3.50←2.50 | 716 433.917 | 18 |
| 36 | *R*( 1) | 1.50←1.50 | 716 437.906 | − 109 |
| 37 | *R*( 1) | 0.50←1.50 | 716 443.796 | 24 |
| 38 | *R*( 2) | 3.50←3.50 | 720 278.934 | − 0 |
| 39 | *R*( 2) | 2.50←1.50 | 720 283.282 | 14 |
| 40 | *R*( 2) | 4.50←3.50 | 720 284.695 | 3 |
| 41 | *R*( 2) | 2.50←2.50 | 720 287.416 | 32 |
| 42 | *R*( 2) | 1.50←1.50 | 720 289.123 | 99 |
| 43 | *R*( 3) | 4.50←4.50 | 724 292.273 | 7 |
| 44 | *R*( 3) | 3.50←2.50 | 724 297.380 | 22 |
| 45 | *R*( 3) | 5.50←4.50 | 724 298.066 | 43 |
| 46 | *R*( 3) | 3.50←3.50 | 724 300.077 | 30 |
| 47 | *R*( 3) | 2.50←2.50 | 724 303.203 | 89 |
| 48 | *R*( 4) | 4.50←3.50 | 728 471.856 | 43 |
| 49 | *R*( 4) | 6.50←5.50 | 728 472.239 | 35 |
| 50 | *R*( 5) | 5.50←4.50 | 732 805.064 | 18 |
| 51 | *R*( 5) | 7.50←6.50 | 732 805.330 | 25 |
| 52 | *R*( 6) | | 737 295.071 | |
| 53 | *R*( 7) | | 741 939.369 | |
| 54 | *R*( 8) | | 746 734.680 | |
| 55 | *R*(10) | | 756 766.394 | 120 |
| 56 | *R*(12) | | 767 361.327 | − 21 |
| 57 | *R*(13) | | 772 859.353 | − 29 |
| 58 | *R*(14) | | 778 484.608 | − 4 |
| 59 | *R*(15) | | 784 231.615 | − 68 |
| 60 | *R*(16) | | 790 094.716 | − 105 |
| 61 | *R*(17) | | 796 067.937 | 124 |
| 62 | $J=1\leftarrow0$ | 2.50←1.50 | 3 358.0900[a] | 0.5 |
| 63 | $J=1\leftarrow0$ | 0.50←1.50 | 3 362.6975[a] | 2.8 |
| 64 | $J=2\leftarrow1$ | 0.50←0.50 | 6 713.3940[a] | 3.1 |
| 65 | $J=2\leftarrow1$ | 0.50←1.50 | 6 723.7560[a] | − 6.5 |
| 66 | $J=3\leftarrow2$ | 1.50←0.50 | 10 067.7320[b] | − 5.7 |

TABLE I (*continued*).

| | | Chlorine-37 measured lines | | |
|---|---|---|---|---|
| I | Line | F′←F″ | OBS (MHz) | OMC (kHz) |
| 1 | *P*(17) | | 674 426.964 | 3 |
| 2 | *P*(16) | | 675 171.423 | 1 |
| 3 | *P*(15) | | 676 053.095 | 27 |
| 4 | *P*(14) | | 677 076.227 | − 30 |
| 5 | *P*(13) | | 678 244.920 | − 27 |
| 6 | *P*(12) | | 679 562.694 | − 16 |
| 7 | *P*(11) | | 681 032.773 | 20 |
| 8 | *P*(10) | | 682 657.940 | 14 |
| 9 | *P*( 9) | | 684 440.819 | |
| 10 | *P*( 8) | | 686 383.464 | |
| 11 | *P*( 7) | | 688 487.704 | |
| 12 | *P*( 6) | 6.50←7.50 | 690 755.234 | 53 |
| 13 | *P*( 6) | 4.50←5.50 | 690 755.424 | 36 |
| 14 | *P*( 4) | 2.50←2.50 | 695 780.660 | 40 |
| 15 | *P*( 4) | 3.50←3.50 | 695 783.098 | 51 |
| 16 | *P*( 4) | 4.50←5.50 | 695 784.660 | 16 |
| 17 | *P*( 4) | 2.50←3.50 | 695 785.180 | 9 |
| 18 | *P*( 4) | 4.50←4.50 | 695 789.213 | 18 |
| 19 | *P*( 3) | 1.50←1.50 | 698 544.699 | − 42 |
| 20 | *P*( 3) | 2.50←2.50 | 698 545.991 | − 49 |
| 21 | *P*( 3) | 3.50←4.50 | 698 548.122 | − 43 |
| 22 | *P*( 3) | 1.50←2.50 | 698 549.252 | − 39 |
| 23 | *P*( 3) | 3.50←3.50 | 698 552.698 | − 17 |
| 24 | *P*( 2) | 1.50←0.50 | 701 470.256 | − 29 |
| 25 | *P*( 2) | 1.50←1.50 | 701 474.795 | − 40 |
| 26 | *P*( 2) | 2.50←3.50 | 701 478.056 | − 31 |
| 27 | *P*( 2) | 0.50←0.50 | 701 478.447 | − 31 |
| 28 | *P*( 2) | 2.50←2.50 | 701 482.620 | − 18 |
| 29 | *P*( 2) | 0.50←1.50 | 701 483.014 | − 15 |
| 30 | *P*( 1) | 1.50←0.50 | 704 570.618 | − 2 |
| 31 | *P*( 1) | 1.50←2.50 | 704 574.260 | − 1 |
| 32 | *P*( 1) | 1.50←1.50 | 704 578.821 | 9 |
| 33 | *R*( 0) | 1.50←1.50 | 711 263.748 | 14 |
| 34 | *R*( 0) | 2.50←1.50 | 711 268.317 | 31 |
| 35 | *R*( 0) | 0.50←1.50 | 711 271.930 | 3 |
| 36 | *R*( 1) | 1.50←0.50 | 714 857.188 | 40 |
| 37 | *R*( 1) | 2.50←2.50 | 714 857.572 | 34 |
| 38 | *R*( 1) | 0.50←0.50 | 714 861.709 | 9 |
| 39 | *R*( 1) | 3.50←2.50 | 714 862.124 | 34 |
| 40 | *R*( 1) | 1.50←1.50 | 714 865.347 | 7 |
| 41 | *R*( 2) | 3.50←3.50 | 718 615.927 | 12 |
| 42 | *R*( 2) | 1.50←0.50 | 718 619.330 | − 10 |
| 43 | *R*( 2) | 4.50←3.50 | 718 620.478 | 11 |
| 44 | *R*( 2) | 2.50←2.50 | 718 622.599 | 9 |
| 45 | *R*( 2) | 1.50←1.50 | 718 623.867 | − 24 |
| 46 | *R*( 3) | 4.50←4.50 | 722 537.304 | − 15 |
| 47 | *R*( 3) | 3.50←2.50 | 722 541.347 | 4 |
| 48 | *R*( 3) | 5.50←4.50 | 722 541.888 | 17 |
| 49 | *R*( 3) | 3.50←3.50 | 722 543.486 | 20 |
| 50 | *R*( 3) | 2.50←2.50 | 722 545.902 | 8 |
| 51 | *R*( 4) | 4.50←3.50 | 726 624.324 | − 29 |
| 52 | *R*( 4) | 6.50←5.50 | 726 624.646 | − 20 |
| 53 | *R*( 5) | 5.50←4.50 | 730 866.752 | − 1 |
| 54 | *R*( 5) | 7.50←6.50 | 730 866.967 | 5 |
| 55 | *R*( 6) | | 735 266.528 | |
| 56 | *R*( 7) | | 739 821.023 | |
| 57 | *R*( 8) | | 744 527.505 | |
| 58 | *R*(11) | | 759 526.724 | − 60 |
| 59 | *R*(12) | | 764 807.060 | − 26 |
| 60 | *R*(13) | | 770 220.456 | 16 |
| 61 | *R*(14) | | 775 761.983 | 48 |
| 62 | *R*(15) | | 781 426.307 | 55 |
| 63 | *R*(16) | | 787 207.592 | − 55 |
| 64 | $J=2\leftarrow1$ | 0.50←1.50 | 6 533.9730[b] | − 0.5 |
| 65 | $J=1\leftarrow0$ | 0.50←1.50 | 3 267.6700[a] | 0.8 |

[a] Reference 17.
[b] Reference 19.

TABLE II. Constants for the ground and Σ bending states of ArHCl.[a]

| | Constant | This work (MHz) | Previous work (MHz) | References |
|---|---|---|---|---|
| Cl-35 | | | | |
| | $\nu$ | 709 223.654(18) | 709 219.96(26) | 24 |
| | $B(000)$ | 1678.5086(25) | 1678.511(5) | 17 |
| | $D(000)$ | 0.019 991(13) | 0.0200(4) | 19 |
| | $H(000)$ | $-4.63(20)\times10^{-7}$ | ··· | |
| | $eqQ(000)$ | ···[b] | −23.0297(5) | 18 |
| | $B(02^00)$ | 1761.3047(27) | 1761.204(53) | 24 |
| | $D(02^00)$ | 0.031 649(15) | ··· | |
| | $H(02^00)$ | $-20.42(26)\times10^{-7}$ | ··· | |
| | $eqQ(02^00)$ | −23.028(93) | −23.84(98) | 24 |
| Cl-37 | | | | |
| | $\nu$ | 707 838.2889(71) | 707 846.9(2.3) | 24 |
| | $B(000)$ | 1631.596 45(88) | 1631.604(5) | 17,19 |
| | $D(000)$ | 0.018 900(6) | 0.0190(4) | 19 |
| | $H(000)$ | $-3.37(14)\times10^{-7}$ | ··· | |
| | $eqQ(000)$ | −18.203(34) | −18.201(50)[c] | 48 |
| | $B(02^00)$ | 1714.604 16(86) | 1711.46(53) | 24 |
| | $D(02^00)$ | 0.030 470(6) | ··· | |
| | $H(02^00)$ | $-20.0(13)\times10^{-7}$ | ··· | |
| | $eqQ(02^00)$ | −18.208(33) | −23.(11.) | 24 |

[a] Errors are $1\sigma$.
[b] Fixed at value of previous work.
[c] Uncertainty estimated by present authors.

near 25 $cm^{-1}$ for ArHCl formed in the planar free jet in argon buffer gas are typically 300–350 kHz FWHM.

Several important advantages clearly result from this Doppler narrowing. The first and most obvious is that this yields a higher resolution spectrum. This also requires, however, that the line be scanned more slowly. Second, as the absorption profile narrows, the peak intensity increases, increasing the sensitivity of the spectrometer. Finally because the absorptions are so narrow, the FM deviation required for full modulation of the absorption is much smaller and therefore the magnitude of base line fluctuations that normally accompany source modulation is greatly reduced.

In addition to line narrowing, Veeken and Reuss[34] and Hagena[49] point out that due to the slower drop in density and temperature in a planar jet expansion ($1/R$ dependence), as compared with the circular nozzle expansion ($1/R^2$ dependence), the extent of clustering is higher in a planar jet. It is not clear whether this is an advantage in the present experiment, as it may result in more extensive formation of larger than desired clusters [e.g., $Ar_n(HCl)_m$ and HCl polymers].

## Beam temperature

In general, it is difficult to obtain accurate relative intensities for many peaks because the sideband power varies considerably as the microwave frequency is swept over large regions. In the case of $ArH^{37}Cl$, $P(2)$ and $P(9)$ fortuitously appeared in the same scan. This occurred because both the upper and lower sidebands are scanned and directed through the jet simultaneously. $P(9)$ appears on the lower frequency sideband, while $P(2)$ appears on the upper sideband at nearly the same microwave frequency (Fig. 4). The sideband responsible for each absorption can be determined by lengthening the FIR laser cavity slightly, thereby shifting the laser frequency slight to the red. This then results in a shift in the microwave frequency at which the absorption occurs, either higher or lower depending on which sideband is being absorbed. The importance of this $P(9)/P(2)$ spectrum is that it provides a ratio of the intensities under approximately identical spectrometer conditions. Using a Fabry–Perot, we were able to determine the actual ratio of the power of the upper sideband to lower sideband. From the corrected ratio of these two peaks a beam temperature of $3(\pm1)$K is obtained. This is not an unreasonable temperature for a circular nozzle; it is, however, colder than expected for a planar jet operating under the present conditions. This is only a

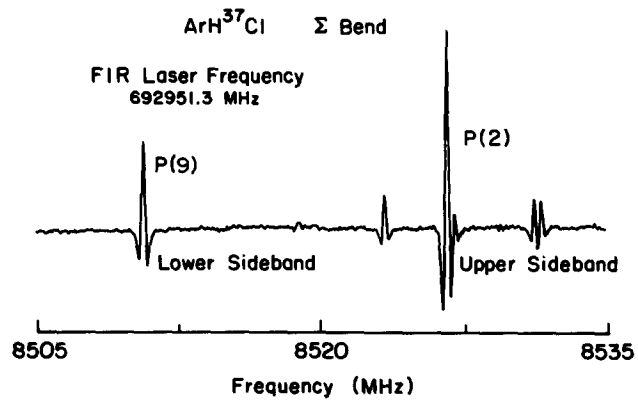


FIG. 4. In this 30 MHz wide scan both $P(2)$ and $P(9)$ of $ArH^{37}Cl$ appear. This results from both the upper and lower sidebands being detected simultaneously. $P(2)$ is on the upper sideband and $P(9)$ is on the lower sideband. This scan gives us an estimate of the jet temperature of 3 K based on the intensities of these two peaks.

single ratio and may not accurately characterize the actual beam temperature, but it certainly does indicate that the expansion is very cold.

### High J splitting

An interesting feature observed in the tunable FIR laser spectra for $J > 15$, is that instead of a single line, a doublet is observed. The width of each line in the doublet is the same as for the low $J$ lines ($\sim 350$ kHz) and the splitting between the lines is approximately the same. The transition out of $J = 16$ produces a broad, flat-topped line, and at higher $J$, the flat top becomes two peaks. As shown in Fig. 5, the transition out of $J = 19$ is a resolved doublet. The signal to noise ratio for these high $J$ transitions is quite low.

We believe that this splitting is due to the incomplete rotational cooling of clusters sampled at the shock wave boundaries of the expansion. The number of cold (3 K) clusters in the main body of the expansion (moving perpendicular to the laser beam) is much greater than the number formed in the shock boundary, therefore only a narrow intense peak is observed for low $J$ transitions. However, for higher rotational quantum numbers, the linewidth increases, indicating that the number of clusters in the shock boundary is becoming comparable to that in the beam; finally, for higher $J$ states the density in the beam becomes still smaller and the dip between the peaks becomes more pronounced. We also find that this splitting does not change significantly with $J$, indicating that these warmer clusters are all found in essentially the same region of the shock. The doublets are very narrow, indicating that the shock boundary region is quite sharply defined.

The information that we can obtain from this data is that there are actually two temperatures associated with the jet, the inner jet temperature, and the shock boundary temperature, which is considerably higher. From the observed Doppler splitting, we can obtain an estimate of the divergence of the planar jet. From the Doppler shift of each peak we find a parallel velocity of 67 m/s. In order to determine the angular divergence of the jet, we need to know the perpendicular velocity of the jet. For pure argon expanded from a circular nozzle a velocity of 560 m/s has been found.[50] Using this value for the perpendicular velocity we obtain $\Theta = 7°$. This angular divergence is obviously quite small compared to that observed with a circular nozzle, which exhibits a broad, cosine-type distribution.[51] Veeken and Reuss have measured a divergence for their pulsed planar jet of 3°.[34]

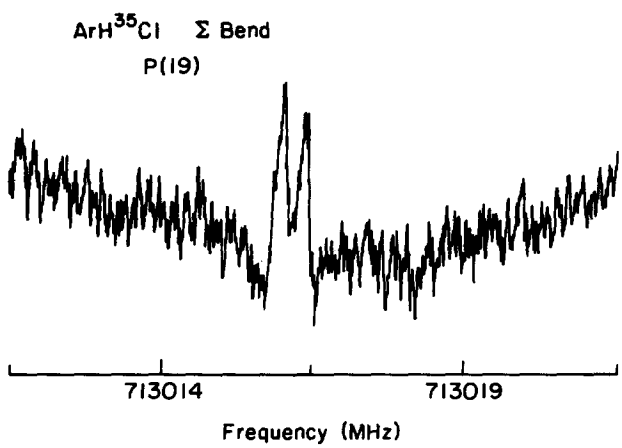


FIG. 5. $P(19)$ of $ArH^{35}Cl$ which shows a splitting characteristic of all the high $J$ scans ($J > 15$). We propose that this splitting occurs because these high $J$ levels are only populated in the warmer boundary regions of the jet, and therefore, are Doppler shifted.

## DISCUSSION

The molecular constants determined from the tunable FIR spectra are presented in Table II, and are compared with the results obtained previously for the Σ bending state and for the ground state. The band origins for both isotopes are shifted from the FIR laser Stark values. A possible explanation for the large difference in band origin $\nu$ for both isotopes is that in the work of Robinson *et al.*,[25] although they were able to measure $P(1)$, they were unable to use it in the fit because the FIR laser frequency had not been accurately determined. Only $R(0)$, $R(1)$, and $R(2)$ were included in the fit. Accurate determination of the band origin without $P$ branch lines is very difficult. The present results are considerably more accurate, as well as more precise, because of the extensive frequency calibrations carried out in this study, the large increase in the number of lines measured, and the reduction in linewidth compared to other FIR techniques.

The recent studies of vibrational spectra of ArHCl were greatly facilitated by the work of Hutson and Howard. By utilizing much of the previously obtained ArHCl data, including line broadening, virial coefficients, scattering, and high resolution microwave spectroscopy, they developed two very different potential surfaces, labeled M3 and M5, both of which fit the available data. The primary difference between these two surfaces is that M5 has a secondary minimum at the ArClH configuration, where M3 does not and is constrained to be flat in this region. Using these two surfaces, the energy levels of the lowest few vibrational states and the associated rotational constants were predicted. Of the lowest three excited states, the Σ stretch, the Σ bend, and the Π bend, the constants associated with the Σ bend most strongly reflect the existence of the secondary minimum. Robinson *et al.* were the first to measure this Σ bend and their results gave strong evidence for this minimum.[24] Our work greatly extends this data set and provides additional constants, particularly the centrifugal distortion constants, which will yield a better characterization of this second well.

From the quadrupole coupling constant we can obtain qualitative information regarding the extent of bending of the complex. The projection of the quadrupole coupling constant on the molecular axis is

$$eqQ_{\mathrm{ArHCl}} = eqQ_{\mathrm{HCl}} \langle P_2(\cos\theta) \rangle,$$

where $\theta$ is the angle between the line connecting the Ar to the HCl center of mass and the HCl molecular axis. This assumes that the quadrupole coupling constant of the HCl subunit is unperturbed in the complex. The constant $eqQ_{\mathrm{HCl}}$ is well determined,[52] and therefore we can determine the value for $\langle P_2(\cos\theta) \rangle$ as 0.3406 for $ArH^{35}Cl$ in the Σ bending state. If we then make the assumption that $\langle \cos\theta \rangle$ is equal to

$\cos\langle\theta\rangle$, we can calculate an approximate average bending angle of either 41.5° or 138.5°, since we cannot rigorously distinguish between an acute or obtuse angle from this measurement. Based on the predictions from Hutson and Howard's M5 potential[29] and calculations of Marshall *et al.* using the BOARS method,[21] it is apparent that the Σ bending state wave function is predominantly localized in the second minimum, i.e., it is closer to the ArClH configuration. The work of Robinson *et al.* strongly favors this description and indicates that the dipole moment for this state is opposite in sign from that in the other low lying vibrational states, implying that the HCl subunit is oriented in the opposite direction. This assumption could not, however, be proven in the Stark experiment, since the sign of the dipole moment could not be determined. On the basis of these prior results, we propose that this angle is the projection on the molecular axis in the ArClH configuration, and is therefore, the obtuse angle. As in the Stark experiment, we cannot prove this assumption. It is interesting to note, however, that the value of $\langle P_2(\cos\theta)\rangle$ is essentially identical in both the Σ bend and the ground state.

The most significant result presented in this article is the development of sensitive, precise, and versatile tunable FIR laser spectroscopy of planar jets as a powerful new technique for detailed investigations of van der Waals interactions. As has been demonstrated recently by Hutson,[53] very accurate anisotropic intermolecular potential surfaces can be determined exclusively from high resolution spectroscopic measurements of the corresponding weakly bound complexes. In particular, Hutson was able to extract a very well-determined surface for ArHCl, conclusively establishing the existence of a secondary minimum (130 $cm^{-1}$ deep) at the ArClH geometry, in addition to the 180 $cm^{-1}$ primary ArHCl well and the 76 $cm^{-1}$ barrier to HCl rotation, exclusively from the measurements of Robinson *et al.*[23–25] of the lowest Π bend, Σ bend, and Σ stretch vibrations and from Pine's determination of the onset of rotational predissociation.[20] Such a detailed description of the van der Waals' potential surface cannot be obtained by any other means. The generality and simplicity inherent in the use of tunable FIR laser spectroscopy for measurement of low frequency vibrational modes in weakly bound complexes will permit spectroscopists to address a wide variety of systems, and should help to advance a new level of detail in our understanding of the nature of intermolecular forces.

## ACKNOWLEDGMENTS

This work was supported by the Director, Office of Energy Research, Office of Basic Energy Sciences, Chemical Sciences Division of the U.S. Department of Energy under Contract No. DE-AC03-76F00098. The FIR laser system was funded by the National Science Foundation (Grant No. CHE-8612296).

[1]D. H. Rank, B. S. Rao, and T. A. Wiggins, J. Chem. Phys. **37**, 2511 (1962).
[2]D. H. Rank, P. Sitaram, W. A. Glickman, and T. A. Wiggins, J. Chem. Phys. **39**, 2673 (1963).
[3]A. W. Miziolek and G. C. Pimentel, J. Chem. Phys. **65**, 4462 (1976).
[4]S. Bratož and M. L. Martin, J. Chem. Phys. **42**, 1051 (1965).
[5]L. F. Keyser and G. W. Robinson, J. Chem. Phys. **44**, 3225 (1966).
[6]M. T. Bowers and W. H. Flygare, J. Chem. Phys. **44**, 1389 (1966).
[7]J. M. P. J. Verstegen, H. Goldring, S. Kimel, and B. Katz, J. Chem. Phys. **44**, 3216 (1966).
[8]D. E. Mann, N. Acquista, and D. White, J. Chem. Phys. **44**, 3453 (1966).
[9]H. Friedmann and S. Kimel, J. Chem. Phys. **44**, 4359 (1966).
[10]W. G. Von Holle and D. W. Robinson, J. Chem. Phys. **53**, 3768 (1970).
[11]E. W. Boom, D. Frenkel, and J. van der Elsken, J. Chem. Phys. **66**, 1826 (1977).
[12]E. W. Boom and J. van der Elsken, J. Chem. Phys. **73**, 15 (1980).
[13]E. W. Boom and J. van der Elsken, J. Chem. Phys. **77**, 625 (1982).
[14]J. M. Farrar and Y. T. Lee, Chem. Phys. Lett. **26**, 428 (1974).
[15]W. B. Neilsen and R. G. Gordon, J. Chem. Phys. **58**, 4149 (1973).
[16]U. Buck and J. Schleusener, J. Chem. Phys. **75**, 2470 (1981).
[17]S. E. Novick, P. Davies, S. J. Harris, and W. Klemperer, J. Chem. Phys. **59**, 2273 (1973).
[18]J. M. Hutson and B. J. Howard, J. Chem. Phys. **74**, 6520 (1981).
[19]S. E. Novick, K. C. Janda, S. L. Holmgren, M. Waldman, and W. Klemperer, J. Chem. Phys. **65**, 1114 (1976).
[20]B. J. Howard and A. S. Pine, Chem. Phys. Lett. **122**, 1 (1985).
[21]M. D. Marshall, A. Charo, H. O. Leung, and W. Klemperer, J. Chem. Phys. **83**, 4924 (1985).
[22]D. Ray, R. L. Robinson, D.-H. Gwo, and R. J. Saykally, J. Chem. Phys. **84**, 1171 (1986).
[23]R. L. Robinson, D. Ray, D.-H. Gwo, and R. J. Saykally, J. Chem. Phys. **87**, 5149 (1987).
[24]R. L. Robinson, D.-H. Gwo, D. Ray, and R. J. Saykally, J. Chem. Phys. **86**, 5211 (1987); R. L. Robinson, D.-H. Gwo, and R. J. Saykally, Mol. Phys. **63**, 1021 (1988).
[25]R. L. Robinson, D.-H. Gwo, and R. J. Saykally, J. Chem. Phys. **87**, 5156 (1987).
[26]S. L. Holmgren, M. Waldman, and. W. Klemperer, J. Chem. Phys. **69**, 1661 (1978).
[27]J. M. Hutson and B. J. Howard, Mol. Phys. **41**, 1123 (1980).
[28]J. M. Hutson and B. J. Howard, Mol. Phys. **43**, 493 (1981).
[29]J. M. Hutson and B. J. Howard, Mol. Phys. **45**, 769 (1982).
[30]J. M. Hutson, J. Chem. Phys. **81**, 2357 (1984).
[31]T. van Dam, A. Rozendaal, J. A. Vliengenthart, and F. B. van Duijneveldt (to be published).
[32]K. L. Busarow, G. A. Blake, K. B. Laughlin, R. C. Cohen, Y. T. Lee, and R. J. Saykally, Chem. Phys. Lett. **141**, 289 (1987).
[33]A. Amirav, U. Even, and J. Jortner, Chem. Phys. Lett. **83**, 1 (1981).
[34]K. Veeken and J. Reuss, Appl. Phys. B **38**, 117 (1985).
[35]C. M. Lovejoy, M. D. Schuder, and D. J. Nesbitt, J. Chem. Phys. **85**, 4890 (1986); C. M. Lovejoy and D. J. Nesbitt, Rev. Sci. Instrum. **58**, 807 (1987).
[36]A. E. Beylich, 12th Int. Symp. on Rarefied Gas Dynamics, p. 710.
[37]M. Sulkes, C. Jouvet, and S. A. Rice, Chem. Phys. Lett. **87**, 515 (1982).
[38]G. Dupeyrat, 12th Int. Symp. on Rarefied Gas Dynamics, p. 812.
[39]D. D. Bićanić, B. F. J. Zuidberg, and A. Dymanus, Appl. Phys. Lett. **32**, 367 (1978); D. D. Bicanić, Int. J. Infrared Millimeter Waves **2**, 247 (1981).
[40]K. M. Evenson, D. A. Jennings, and F. R. Petersen, Appl. Phys. Lett. **44**, 576 (1984).
[41]J. Farhoomand, G. A. Blake, M. A. Frerking, and H. M. Pickett, J. Appl. Phys. **57**, 1763 (1985).
[42]G. A. Blake, K. L. Busarow, R. C. Cohen, K. B. Laughlin, Y. T. Lee, and R. J. Saykally, J. Chem. Phys. (submitted).
[43]R. C. Cohen, K. L. Busarow, K. B. Laughlin, G. A. Blake, Y. T. Lee, and R. J. Saykally J. Chem. Phys. (submitted).
[44]K. B. Laughlin, G. A. Blake, R. C. Cohen, D. C. Hovde, and R. J. Saykally, Philos. Trans. R. Soc. London Ser. A **324**, 97 (1987).
[45]M. Ignuscio, G. Moruzzi, K. M. Evenson, and D. A. Jennings, J. Appl. Phys. **60**, R161 (1986).
[46]H. P. Röser, E. J. Durwen, R. Wattenbach, and G. V. Schultz, Int. J. Infrared Millimeter Waves **5**, 301 (1984).
[47]F. C. DeLucia, P. Helminger, and W. Gordy, Phys. Rev. A **3**, 1849 (1971).
[48]E. J. Campbell and W. G. Read, J. Chem. Phys. **78**, 6490 (1983).
[49]O. F. Hagena, Surf. Sci. **106**, 101 (1981).
[50]R. B. Bernstein, *Chemical Dynamics via Molecular Beam and Laser Techniques*, 1st ed. (Oxford, New York, 1982), p. 32.
[51]Y. Mizugai, H. Kuze, H. Jones, and M. Takami, Appl. Phys. B **32**, 43 (1983).
[52]E. W. Kaiser, J. Chem. Phys. **53**, 1686 (1970).
[53]J. M. Hutson, J. Chem. Phys. (accepted).